DRAFT VERSION AUGUST 18, 2017
Preprint typeset using LaTeX style emulateapj v. 11/10/09

IMPACT OF PROTON-PROTON NUCLEAR REACTION IN THE EVOLUTION OF A POST-MAIN SEQUENCE STAR

GONÇALO ANDRADE [1], ILÍDIO LOPES [1]

Draft version August 18, 2017

ABSTRACT

We investigate how the different S-factors for the $p(p, e^+\nu_e)^2H$ nuclear reaction rate impact the evolution of a fiducial star with 1.5 solar masses in a critical stage in the post main-sequence phase. Using high-precision stellar evolution models, with three different S-factors published in the literature, we show that the stellar structure is particularly sensitive to the change in this stage of evolution. Stars with masses of 0.9 and 7.0 $M_\odot$ also show some sensitivity to this nuclear reaction.

For the fiducial star, we have yielded a maximum difference of about 1.3μHz between $\Delta\nu_{n,l}$ vs $\nu_{n,l}$ curves for radial modes in the same phase of stellar evolution, an analysis that could allow us to make a clear distinction between some of the different S-factors if the mean error in the eigenfrequencies were smaller or about 0.65μHz. The conditions for which this measurability occurs arise specifically near the red giant phase of the evolution, before and after which such differences become much smaller, and the effects seem to be maximum in a phase where the transport of energy is dominantly radiative.

Subject headings: asteroseismology – nuclear reactions, nucleosynthesis, abundances – stars: general – stars: evolution – convection – radiation mechanisms: general

1. INTRODUCTION

Stars are among the most important components of the universe and the comprehension of the physical processes occurring inside them is of fundamental importance to understand the formation of larger structures such as stellar clusters, galaxies and galaxy clusters. Indeed, to follow the formation and evolution of our universe, and to be able to accurately predict its present structure is paramount to understand in great detail the network of nuclear reactions occurring in stars. The mechanism responsible for the energy production in stellar objects was an enigma to astrophysicists until the first quarter of the XX century with the discovery of Einstein's relation between mass and energy (Einstein 1905) and the proposal by Sir Arthur Eddington that the energy source of the Sun was due to the conversion of mass into energy through the fusion of Hydrogen into Helium (Eddington 1920).

It turned out that Eddington's proposal was right, Bethe (1939) investigated several possibilities of nuclear reactions, concluding that the proton-proton (pp) chain and carbon-nitrogen-oxygen (CNO) cycles were the main source of energy for stars, at least during the main-sequence (MS) phase. This fact gives us a hint that knowing the efficiency of these reactions should have a critical impact on the predictions we can make about stellar structure and evolution.

Nuclear reaction rates usually are represented by means of a parameter, the so-called S-factor, which can be either computed from theory or measured experimentally, and differs from nuclear reaction to nuclear reaction. Specifically, the S-factor captures how the nuclear structure of the reacting nuclei impacts the reaction's cross-section. In section 2.1 this term will be explained in more detail.

In recent years, the interest of asteroseismology has been on the rise as a method for probing stellar interiors, since it allows an independent observational test of stellar models (e.g. Unno et al. 1989; Gough 1985). The recent missions CoRoT (Baglin et al. 2006) and Kepler (Gilliland et al. 2010; Koch et al. 2010) have gathered data from the oscillations of several stars. For instance, the Kepler mission has acquired high-quality long-cadence data for about 14×10^3 red-giants with uninterrupted coverage in the first 3.5 years of mission (e.g. Chaplin & Miglio 2013). Moreover, this data availability is going to increase even further in the future, with the new ESA and NASA's missions PLATO (Rauer et al. 2014) and TESS (Ricker et al. 2015), the second of these new missions is predicted to monitor more than 2×10^5 stars (Ricker et al. 2014). As we argue in this work, these large amounts of high-quality astereoseismic data may allow us to validate and constrain the nuclear reactions occurring in the core of stars, a particularly interesting aspect since these nuclear reactions operate in extreme thermodynamic conditions which are currently impossible to replicate on Earth's laboratories. In many cases it may be the only way possible to validate the theoretical computation of a nuclear reaction, as is currently the case for the one considered in this study.

Currently, nuclear physics laboratories are quite successfully measuring the S-factor of many nuclear reactions, and from time to time all these results are compiled and published in leading articles where the recommended values to be used in nuclear astrophysics are presented (e.g., Caughlan & Fowler 1988; Angulo et al 1999). The $p(p, e^+\nu_e)^2H$ is one of the main reactions responsible for the evolution of any star in the main-sequence, greatly influencing its life but, unlike many others, its cross section is too small to be measured in the laboratory and has to be calculated from the standard weak interaction theory (e.g. Adelberger et al. 2011). In this article, we will call that reaction simply the pp reaction, if not stated otherwise.

The calculation of the pp reaction has an associated uncertainty that can produce some changes in stellar models and some authors have argued that the current uncertainty in the value of the pp reaction's S-factor is not enough to produce significant changes in the structure of MS solar-like stars.

[1] Centro Multidisciplinar de Astrofísica, Instituto Superior Técnico, Universidade de Lisboa, Av. Rovisco Pais, 1049-001 Lisboa, Portugal; goncalo.andrade@tecnico.ulisboa.pt , ilidio.lopes@tecnico.ulisboa.pt

TABLE 1
TABLE WITH DIFFERENT S-FACTORS OF THE PROTON-PROTON NUCLEAR REACTION AVAILABLE IN THE LITERATURE.

Model [a]	$S(0)$ MeV b	$S'(0)/S(0)$ MeV^{-1}	$S''(0)/S(0)$ MeV^{-2}	Source
Ref (NACRE)	3.94×10^{-25}	11.7	75 ± 10	Angulo et al (1999)
	$(3.99 \pm 0.14) \times 10^{-25}$	11.3 ± 0.1	170 ± 2	Chen et al. (2013)
	$(4.01 \pm 0.04) \times 10^{-25}$	11.2 ± 0.1	-	Adelberger et al. (2011)
	$(4.047^{+0.024}_{-0.032}) \times 10^{-25}$	10.84 ± 0.02	317.8 ± 1.3	Acharya et al. (2016)
A	$(4.081^{+0.024}_{-0.032}) \times 10^{-25}$	10.84 ± 0.02	317.8 ± 1.3	Acharya et al. (2016)
B	$(4.033 \pm 0.003) \times 10^{-25}$	12.23 ± 0.01	178.4 ± 0.3	Marcucci et al (2013)

[a]S-factors without a label were not used in the simulations.

These errors do not impact the time that the star is in the MS phase, meaning that it produces no relevant changes in the determination of the age of globular clusters (e.g. Brocato et al. 1998; Tognelli et al 2015), and we confirm this with our results.

In this article we will analyze the impact that the current uncertainty in the $p(p, e^+\nu_e)^2H$ reaction has in the structure of post MS stars, namely the changes produced in the large separation of radial modes. We will also show that the sensitivity to the S-factor of this reaction will be particularly important in critical stages of the stellar evolution discussed in this work. In particular, if these changes are measurable with the current precision of asteroseismology data, or if it can be done in the future with the forthcoming high-quality measurements expected to be attain by the next generation of asteroseismic missions.

This paper is organized in 4 sections: the present section where we have made a short introduction to this work (1), a second section (2) in which we discuss in some detail the standard parametrization of nuclear reactions used in stellar astrophysics, and a third section (3) where we present and discuss the main results of our work. The final section (4) presents our main conclusions.

2. THE CRITICAL NUCLEAR REACTION PROTON PROTON AND THE EVOLUTION OF RED GIANT STARS

2.1. *The nuclear proton proton reaction*

To analyze the impact of a given reaction on the structure of the star, we are required to know that the cross-section of the nuclear reaction $\sigma(E)$ defines the probability of occurrence of that reaction as a function of the energy E on the center of mass (CM). It is convenient, however, that one considers another function $S(E)$ called the Astrophysical factor or S-factor (e.g. Kippenhahn et al. 2012), that relates it with the cross section by

$$\sigma(E) = S(E)\exp(-2\pi\eta)\frac{1}{E}, \tag{1}$$

since this function is well behaved compared with most cross-sections (e.g. Angulo et al 1999). The factor η is the Sommerfeld parameter and is defined by

$$\eta = \frac{Z_1 Z_2 e^2}{\hbar v} = \frac{0.9895}{2\pi} Z_1 Z_2 \left(\frac{A}{E}\right)^{1/2}, \tag{2}$$

where Z_1 and Z_2 are the charge numbers of the interacting particles, e is the elementary charge, $\hbar$ is the reduced Plack constant, v is the relative speed, A is the system's reduced mass in atomic mass units and E is the kinetic energy available in the CM.

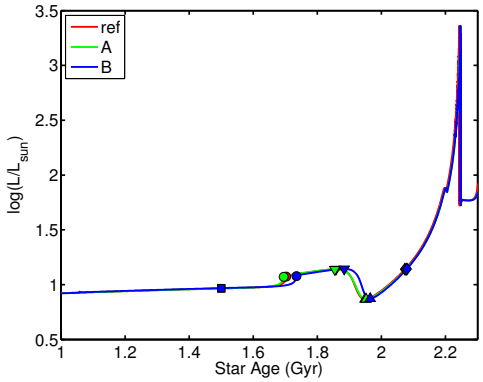

FIG. 1.— Plot of base 10 logarithm of stellar luminosity as a function of the age. Each color denotes stellar models evolved with different S-factors from table 1. The squares **(1)**, circles **(2)**, down-triangles **(3)**, up-triangles **(4)** and the diamonds **(5)** denote critical points **1** to **5** explained in subsection 2.2.

The S-factor is then a function introduced which connects the expression for a simple quantum tunnelling model with the actual cross-section by including all the details of how the nuclear structure of the nuclei impacts it. It can be determined experimentally by measuring $\sigma(E)$ or, in cases where this value cannot be measured, it can be theoretically calculated using, for instance, standard weak interaction theory. However, this theoretical approach implies a greater uncertainty in the obtained values. The S-factor is usually expressed through a measured table and well approximated by a polynomial function (e.g. Marcucci et al 2013)

$$S(E) \simeq S(0) + S'(0)E + S''(0)E^2/2 + \cdots, \tag{3}$$

and table 1 shows these components, $S(0)$, $S'(0)$ and $S''(0)$, as they have been estimated for the pp reaction by the cited authors. Our reference model is based on the recommended values of the NACRE compilation (Angulo et al 1999) while our model **A** uses Acharya et al. (2016) results, obtained using chiral effective field theory (χEFT) up to next-to-next-to-leading order, and our **B** model (Marcucci et al 2013) does an analysis also based on χEFT but considers the full electromagnetic interaction, including, beyond Coulomb, two-photon and vacuum-polarization corrections. For completeness other S-factor values found in the literature are also shown in the table.

The first stage of the proton-proton (pp) chain is arguably the most important reaction in the context of stellar evolution, it is the step that enables other reactions to take place and is characterized by the diagram $p(p, e^+\nu_e)^2H$, the fusion of two protons in a deuterium, also expelling a positron and an electronic neutrino.

Even though the first pp reaction is known from a theoret-

ical point of view, its use raises a problem because it is not possible to measure its cross-section on terrestrial laboratories (e.g. Marcucci et al 2013), giving rise to larger uncertainties on the rates' values. Solar-like stars, for example, have a core temperature about 1.5×10^7 K and a Gamow peak of about 6 keV, for which the cross-section is too small to be detected (e.g. Adelberger et al. 2011).

The impact that this leading pp chain reaction has in the stellar structure has been recently studied for the Sun and for the determination of the age of globular clusters, for instance by Tognelli et al (2015), which concludes that the current uncertainty does not impact significantly this kind of structures, predictions that are confirmed by our results.

After the main-sequence phase, when the hydrogen in the center is consumed, the stellar core contracts and the envelope expands. In the meantime, the conditions where burning of Hydrogen occurs become more extreme, with most reactions occurring in a thin shell outside an inert Helium rich core through the CNO cycle.

The S-factor influences the description of the pp reaction since it determines the nuclear reaction rates on the various stellar environments, which influence not only the local energy production but also change the chemical composition of the star. This relation is given by (e.g. Angulo et al 1999; Kippenhahn et al. 2012)

$$N_A\langle\sigma\nu\rangle = N_A \frac{(8/\pi)^{1/2}}{A^{1/2}(k_B T)^{3/2}} \int_0^\infty \sigma(E).E.e^{-E/k_B T} dE\,, \tag{4}$$

where N_A is the Avogadro constant, $\langle\sigma\nu\rangle$ is the probability per unit of time that two particles, confined in a unit volume, react with each other through the correspondent reaction, and k_B is the Boltzmann constant. This equation relates directly with the S-factor through equation 1.

The evaluation of this expression is a determinant factor to compute the evolution of a star, since it gives us the probability of a reaction occurring per particle density and unit volume, predicting the energy production inside the star. This evaluation was done using an approximation method (e.g. Bahcall 1989; Adelberger et al. 1998, 2011) tested in codes of stellar evolution like CESAM (Morel & Lebreton 2008).

2.2. *Star in the post-main sequence phase*

To analyse the impact of the changes in the pp reaction, we opted by choosing well defined steps of the evolution of the star. Moreover we start by choosing a fiducial star with $1.5M_\odot$, close to KIC 8026226 for which there is already some asteroseismology data and discussion (Appourchaux et al. 2012; Molenda-Żakowicz et al. 2013).

To compute stellar models, we use a stellar evolution code called MESA (version 8845, Paxton et al. 2011, 2013, 2015), a modular code that allows the creation of a stellar structure model at a certain age by simulating the evolution of the star until that age. We use the default template to compute the time evolution of one solar mass star from the pre-MS until the white dwarf phase and changed only the following parameters: **(i)** the stellar mass, mixing length (α) and initial H (X_0) and He (Y_0) abundances, **(ii)** all nuclear reactions were set to use the Angulo et al (NACRE, 1999) values, and **(iii)** in the case of the first reaction of the pp chain – $p(p, e^+\nu_e)^2H$, the reaction rate was changed to use the S-factors from table 1. The simulation of this star was stopped shortly after the Helium flash and, for the parameters in **(i)**, we adopted the values

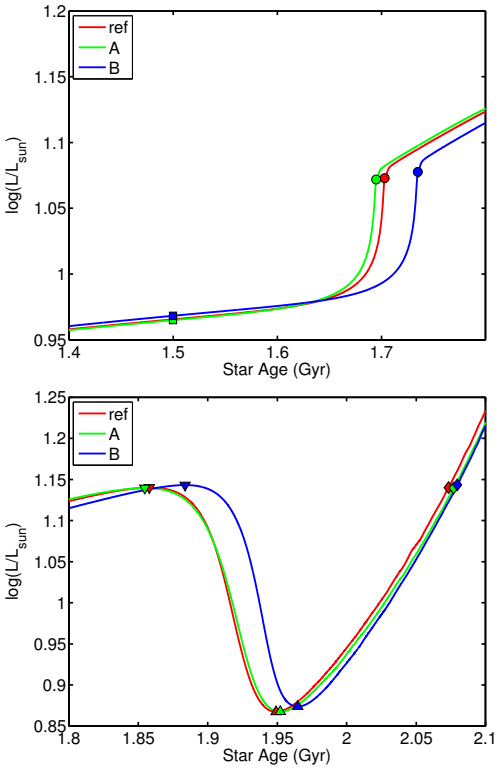

FIG. 2.— These figures show the same information as figure 1, but with a zoom near the critical points for better visibility. The squares **(1)**, circles **(2)**, down-triangles **(3)**, up-triangles **(4)** and the diamonds **(5)** denote critical points **1** to **5**.

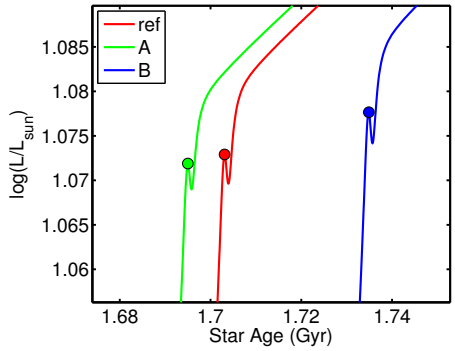

FIG. 3.— Plot of base 10 logarithm of stellar luminosity as a function of the age. Each color denotes stellar models evolved with different S-factors from table 1. Detail on points **(2)** from figure 1.

obtained by Metcalfe et al. (2014), which are available in the website Asteroseismic Modeling Portal (AMP 2014), if not otherwise stated.

After computing the stellar models in MESA, a stellar oscillation code called GYRE (version 5.0, Townsend & Teitler 2013) was used to compute the radial oscillations of different equilibrium structures of the star at different stages of the star's evolution. This code uses the output stellar models from MESA and allows us to choose a range of frequency in which it searches for natural frequencies.

We have chosen five bench models at distinct phases of the evolution, these models are shown in figures 1, 2 and 3, and the main parameters of the star at these critical points of evolution for the different values of the pp reaction (see table 1) can be seen in table 2. They were chosen using the following

TABLE 2
TABLE WITH THE DIFFERENT S-FACTORS CONSIDERED IN THE MODELS. ALL THE MODELS USE AN INITIAL MASS OF $1.5M_{\odot}$, A $Y_0 = 0.247$, $Z = 0.01253$ AND THE MIXING LENGTH $\alpha = 1.28$, ACCORDING TO THE BEST MODEL PARAMETERS FOR KIC 8026226 FROM METCALFE ET AL. (2014). Y_0 AND Z REPRESENT RESPECTIVELY THE MASS FRACTION OF ^{4}HE AND ELEMENTS HEAVIER THAN He IN THE INITIAL MODEL, X_c AND Y_c REPRESENT THE CENTER ABUNDANCE OF ^{1}H AND ^{4}HE IN THE CORRESPONDENT MODEL.

Model Id	$R/R_{\odot}$	$L/L_{\odot}$	T_{eff} (K)	Age [a] (Gyr)	m_{bcz}/M_{star}	$\Delta\nu_{0n}$ (μHz)	X_c	Y_c
Ref1	1.940	9.237	7228.9	**1.500**	-	58.287	0.1660	0.8217
Ref2	1.940	11.83	7690.9	1.703	-	58.041	0.0005	0.9872
Ref3	2.826	13.80	6623.2	1.858	-	33.950	$< 10^{-4}$	0.9878
Ref4	3.875	7.369	4834.7	1.949	0.743	22.212	$< 10^{-4}$	0.9878
Ref5	5.884	13.80	4589.9	2.073	0.239	11.745	$< 10^{-4}$	0.9878
A1	1.942	9.224	7223.8	**1.500**	-	58.233	0.1601	0.8276
A2	1.930	11.80	7705.9	1.695	-	58.373	0.0005	0.9872
A3	2.812	13.79	6637.8	1.855	-	34.175	$< 10^{-4}$	0.9878
A4	3.876	7.373	4834.7	1.952	0.743	22.203	$< 10^{-4}$	0.9878
A5	5.879	13.79	4590.6	2.077	0.240	11.759	$< 10^{-4}$	0.9878
B1	1.924	9.295	7270.5	**1.500**	-	58.946	0.1888	0.7989
B2	1.971	11.96	7650.2	1.735	-	56.734	0.0005	0.9873
B3	2.893	13.90	6557.1	1.884	-	33.056	$< 10^{-4}$	0.9878
B4	3.908	7.477	4831.8	1.965	0.741	21.986	$< 10^{-4}$	0.9878
B5	5.908	13.91	4589.1	2.080	0.240	11.667	$< 10^{-4}$	0.9878

[a]All age take into account the evolution of the star in the pre-MS phase.

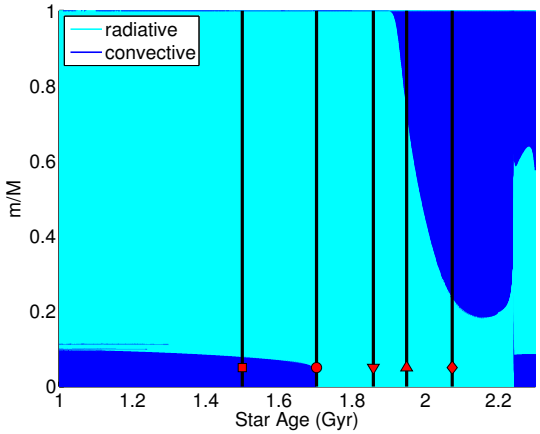

FIG. 4.— Kippenhahn plot of the reference star model (**Ref**) where the colors represent convective and radiative mixing. Black vertical lines mark the age of the bench models for that same star and the markers at the bottom of those lines use the same nomenclature as the points in figure 1 to identify the model, i.e. they all belong to the **Ref** model.

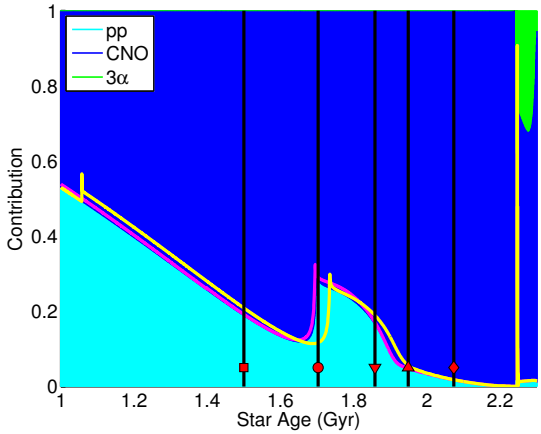

FIG. 5.— The present figure represents the total energy produced in the star for pp chain, CNO cycle and triple-alpha reactions divided by the sum of the three. The cyan, blue and green zones correspond to the contributions in the Ref model, while the magenta and yellow lines correspond to the "frontier" between the pp chain and CNO cycle for models **A** and **B**, respectively. Black vertical lines use the same system as in figure 4.

criteria:

- the bench models **(1)** and **(5)** were chosen as representative stages of the evolution of the star: model **(1)** corresponds to a 1.5 Gyr star in the main-sequence, for which the evolution of the star is dominated by the production of energy in the core by the pp-chain and the CNO cycle, with the energy evacuation being done through radiative outer layers (square in figures 4 and 5); and model **(5)** corresponds to a star in the red giant phase[2], a phase of stellar evolution where the production of energy becomes dominated only by the CNO cycle, and the star has a large external convective envelope that includes most of the star's mass (diamond in figures 4 and 5).

- the bench models **(2)**, **(3)** and **(4)** were chosen at critical stages of the evolution of the star: model **(2)** at the end of the MS, in which the star loses its convective core (circle in figures 4 and 5) and the luminosity curve displays a characteristic feature (figure 3); model **(3)** a local maximum of the luminosity in the post MS phase (down-triangle in figures 4 and 5) for which the star is fully radiative; and model **(4)** a local minimum of the luminosity also in the post MS phase (up-triangle in figures 4 and 5), in which the star has a radiative core and an already important convective envelope.

More important, all those critical stages of the evolution of the star have a significant impact in the asteroseismic properties, namely the large separation of the star, as can be seen in figures 6 and 7.

2.3. *Asteroseismology of post-main sequence stars*

Asteroseismology is a field in astrophysics that uses stellar oscillations as a method to investigate the internal structure of stars, providing important clues for stellar physics and evolution. It's possible to understand that the eigenfrequencies of stellar bodies are influenced by their constitution, and it's pos-

[2] This point was chossen with the same luminosity as bench point **(3)**.

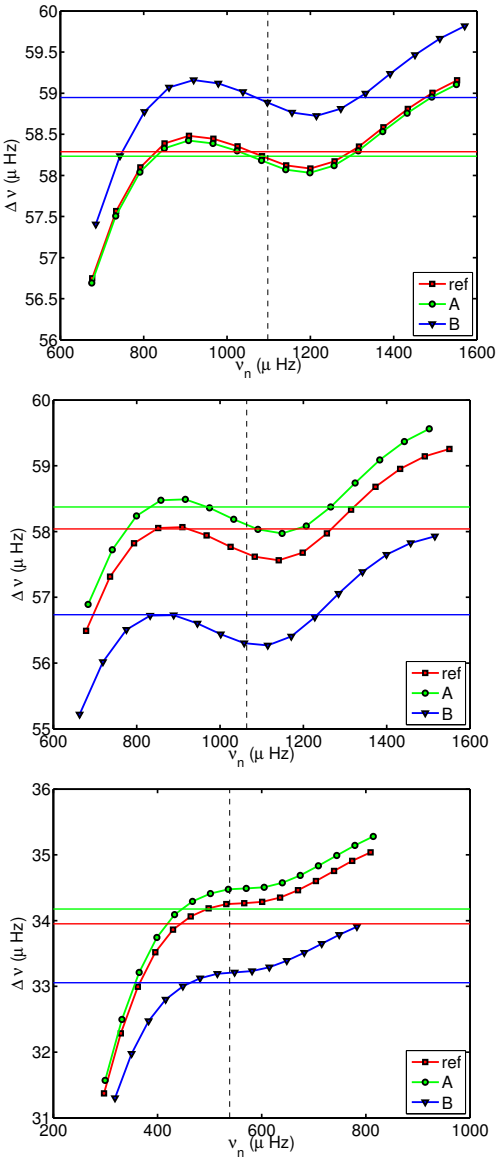

FIG. 6.— Large separation ($\Delta\nu_{n,0}$) as a function of the frequency ($\nu_{n,0}$) for bench points **1** (top), **2** (middle) and **3** (bottom). Different colors identify different models, each associated with a different S-factor. The horizontal line represents the mean value of the large separation for the selected set of data and has the color associated with its model and the vertical dashed line is the estimated ν_{max} value through equation 8 for the reference model.

sible to use both the absolute values of the frequencies or the relationships between frequencies of different modes to make a diagnostic about some specific parts of the star.

The process through which the stellar oscillations are excited still require further investigation since solar-like oscillations are usually stochastically excited by instabilities due to the existence of a convective envelope (e.g. Antoci 2014), in a process that excites all frequencies in a given range. Most oscillations are then damped and only the modes compatible with the star's eigenfrequencies survive. However, bench models **(1)**, **(2)** and **(3)** have no or negligible convective envelopes in terms of the mass of the star, as can be seen in figure 4, which may raise the question of how the oscillations are triggered. Even though our analysis focus on the value of the eigenfrequencies, which is not changed by this problem, this is a relevant question for the problem of observability.

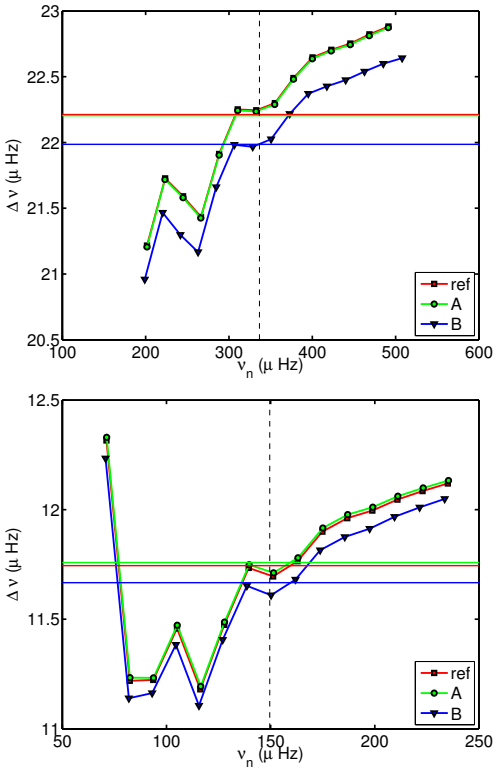

FIG. 7.— Large separation ($\Delta\nu_{n,0}$) as a function of the frequency ($\nu_{n,0}$) for bench points **4** (top) and **5** (bottom). The nomenclature is the same as in figure 6.

Some authors have used experimental asteroseismic data to model similar stars (e.g. Metcalfe et al. 2014), and there are several mechanisms, known to be part of the excitation process in other stars, that could be at least part of the cause of these oscillations, namely instabilities due to the κ-mechanism (e.g. Eddington 1919; Cox 1963), the ϵ-mechanism (e.g. Glatzel & Kiriakidis 1993), the existence of mass negligible sub-surface convective zones (e.g. Cantiello et al. 2009) or even, in bench points **(1)** and **(2)**, instabilities due to the convective core.

It is likely that some of those excitation types will be in part responsible for the stimulation of stellar oscillations in the post MS phase. As such in this study we will assume that some form of excitation is driving oscillations, nevertheless we will be focused only in the variation of eigenfrequencies with structure due to the changes of the S-factor of the pp nuclear reaction.

A star of $1.5M_{\odot}$ in the post MS phase, such as the one in this study, has the potential to have acoustic, gravity and mixed modes (e.g. Unno et al. 1989; Carrier et al. 2005; Deheuvels & Michel 2011) but, in this work, we will focus only on the impact of the pp chain in the radial modes for two main reasons. First, the radial modes are very penetrating modes in the stars and therefore can be sensitive to the properties occurring in the core. Second, acoustic modes are very well understood in terms of the theory of stellar pulsations, which facilitates the interpretation of our results. A detailed account about the properties of acoustic modes can be found in the literature (e.g. Tassoul 1980; Unno et al. 1989; Gough et al. 1993; Lopes 2001).

We compared the large separation of the bench models to check if the differences were measurable. This quantity can

be defined by (e.g. Chaplin & Miglio 2013)

$$\Delta\nu_{n,l} = \nu_{n,l} - \nu_{n-1,l} \approx \nu_0 \tag{5}$$

where l is the angular degree of the mode, n is the radial degree, $\nu_{n,l}$ is the frequency of the eigenmode (n,l) and ν_0 is the approximate constant value of this quantity, a very important parameter that has a relationship with the radius of the star given by

$$\nu_0 = \left(2\int_0^R \frac{dr}{c}\right)^{-1} \tag{6}$$

where R is the radius of the star, r is the radial coordinate and c is the sound speed as a function of r. However, this is just an approximation, and we can see in figures 6 and 7 how this quantity differs for radial modes ($l = 0$) as a function of $\nu_{n\,0}$ in the same bench model. This variation in $\Delta\nu_{n,0}$ is due to the changes occurring in the external layers of the star (Lopes & Turck-Chieze 1994; Lopes & Gough 2001; Brito & Lopes 2017).

To determine the boundaries of the frequency values to use in the eigenfrequencies' calculation we used stellar scalling relations, a set of expressions that can be used to estimate how certain quantities change knowing how other quantities have changed relative to some known star's set of parameters (usually the Sun). The relations used were (e.g. Belkacem et al. 2013; Mosser 2015)

$$\frac{\nu_0}{\nu_{0,\odot}} = \left(\frac{M}{M_\odot}\right)^{1/2}\left(\frac{R}{R_\odot}\right)^{-3/2} \tag{7}$$

$$\frac{\nu_{max}}{\nu_{max,\odot}} = \left(\frac{M}{M_\odot}\right)\left(\frac{R}{R_\odot}\right)^{-2}\left(\frac{T_{eff}}{T_{eff,\odot}}\right)^{-1/2} \tag{8}$$

where the $\odot$ symbol denotes a Solar quantity, and they are valid for evolutionary stages from the MS to the He-core burning phase of Red Giants (Huber et al. 2011) [3]. Using these equations to estimate $\Delta\nu$ and ν_{max} for the **Ref** S-factor in each bench model, the frequency boundaries considered were $\sim (\nu_{max} \pm 8\nu_0)$, which were used for the three different S-factor models at the same stage.

3. RESULTS AND DISCUSSION

By analyzing the simulation results in the presented tables and figures, we conclude that they show a sensitivity of the stellar structure to the S-factor, namely in the post-MS phase.

In figure 1 we see that the overall time of each phase of evolution almost doesn't change, with luminosity curves that overlap for almost all ages. The only regions where there is a bigger difference are near and between bench models **(2)** and **(4)** and, remarkably, our simulations hint that after this phase the two curves again almost coincide, having the same shape and no age shift, even though we can clearly see a difference in the age of the selected models from **(2)** to **(4)**.

The impact of the S-factor in the stellar models causes observed differences in $\Delta\nu_{n,l}$ mean value (equation 5) and thus in ν_0, which can be related to the stellar radius through equation 6. In fact, by comparing the values in table 2, we can see that the changes in percentage of ν_0's values relative to the Ref models have a strong linear[4] correlation with the correspondent changes in R and, as expected, when R increases, ν_0 decreases and vice-versa.

Another obvious difference between different models is that the first three groups of points have almost completely radiative envelopes (see figure 4), while in the last two groups a large convective envelope appears, a difference that has an important impact in the large separation of the star, as can be seen by comparing figures 6 and 7. This distinct difference is possibly a manifestation of the fact that in the models with convective envelopes (figures 4 and 7) the star can have a region of partial ionization of Helium, like is found in some MS stars (Brito & Lopes 2017), something that does not occur in the cases where stars have radiative envelopes, see figure 6.

When looking at different points in the same group, if we consider the age of bench model number **(2)** from table 2, we can see they are very close both in terms of age, the relative difference with respect to the reference model is about -0.47% for model **A** and 1.88% for model **B**, and general parameters. There is a tendency of **A** values being closer to the **Ref** than **B** values that was prevalent over the generality of analyzed parameters from the referred table. For instance, the mean values of the large separation for **A2** and **A3** were 0.57% and 0.66% bigger than the correspondent **Ref** values while in **B** they are, respectively, 2.3% and 2.6% smaller than **Ref**. Other parameters' differences are usually of the order of 0.15% for model **A** and 1% in model **B**, although this varies substantially.

A very important point to analyze is the difference caused by the change in the S-factor when the luminosity reaches a local maximum in points **(2)** and **(3)** referred in the last paragraph. These are the ones with bigger differences in all parameters. Comparing, for instance, figure 6's top plot with the middle and bottom plots we can see important changes in the differences' magnitudes. In the first one, **Ref** and **A** curves are really close, less than 0.06μHz apart, and the **B** curve is only about 0.7μHz apart from the other two. If we could find and measure such a star, these differences would be indistinguishable if the error in the measurement of each frequency was about 0.35μHz because, to calculate the large separation, the error sums up so if we have two modes with this mean error, it already makes a large separation error of 0.7μHz, the difference between the curves. A higher precision would allow the distinction between **B** and the other two models, but could not differentiate **A** from **Ref**, since this difference, according to the data in table 2, is of the order of 0.06μHz and would thus require a 0.03μHz mean error. In critical points **(2)** and **(3)**, the difference in the large separation is much more intense and, in point **(2)**, is about 0.2μHz between **Ref** and **A** curves and 1.3μHz between **Ref** and **B**, with the **Ref** model in the middle of the two modified curves. If this prediction is correct, even though **A** and **Ref** have a smaller difference that would require an average error of 0.1μHz in the frequencies, **Ref** and **B** have a larger distance and could, in principle, be distinguished with a mean observational error of 0.65μHz. Point **(3)** has similar results, also with about 0.2μHz between **Ref** and **A** and about 0.9μHz between **Ref** and **B**, requiring an average error of 0.1μHz and 0.45μHz to make the distinctions.

The third bench point has also another advantage. By looking at the bottom of figure 6 we can also notice the pattern of

[3] The cited reference does not show this for equations 7 and 8 but for other ones that can easily be shown to be equivalent, provided that $L \propto R^2T^4$.

[4] Note that the changes are small.

the large separation being much more flat than the pattern in the top and bottom plots and in both figure 7 plots. A further analysis on the evolution of this pattern with the age of the star and on the explanation of it still needs to be done but, if this flatness shows up to be unique of this stage, the pattern could be used to identify stars in this luminosity local maximum.

After critical point **(3)**, a new pattern arises in the large separation, which can be seen in figure 7 plots and a closer look on critical points **(4)** and **(5)** reveals that the difference between the models is now much smaller than in critical point **(3)**, reduced (in point **(4)**) to about 0.01μHz between **Ref** and **A** and 0.2μHz between **Ref** and **B**, making it much harder to distinguish between the curves.

The precisions required to measure the differences in some of the critical points will possibly be achieved by the new missions PLATO and TESS. According to Libbrecht (1992) formula,

$$\sigma_\nu^2 = f(\beta)\frac{\Gamma}{4\pi T} \tag{9}$$

where σ_ν is the error in the frequency, Γ is the Full Width at Half Maximum (FWHM) linewidth (proportional to the damping rate of the mode), T is the observation time and

$$f(\beta) = (1+\beta)^{1/2}[(1+\beta)^{1/2} + \beta^{1/2}]^3 \tag{10}$$

with $\beta = (STN)^{-1}$, being the inverse Signal-to-Noise ratio. This analysis is valid at least when the modes are stochastically excited.

Based on some of Lochard et al. (2005) values, for modes with short lifetimes, a quick evaluation where we consider STN ~ 9 and $\Gamma \sim 4.3 \times 10^{-2}\mu$Hz, yields that the observation time required to obtain a 0.45μHz uncertainty on the frequencies would be about 5.5 days. However, this depends heavily on the specific characteristics of each target, namely the lifetime of the mode and the achieved signal-to-noise ratio, and on the range of evaluated frequencies.

While our current knowledge of the mechanism that links the change in the S-factor to the observed changes in the post MS phase is still progressing, it is worth mentioning two points. On one hand, by looking at the Kippenhahn plot 4, we can see that the luminosity plateau, where most changes were observed, is a region where the star's energy transport is dominated by the radiative process. This kind of transport is known to be less effective than convection when the stellar material opacity is high (Ryan & Norton 2010), which might help accumulate energy inside the star causing bigger differences if the rate of energy production is different. On the other hand, these small changes have also a small effect on the competition between the pp chain and the CNO cycle, as can be observed in figure 5. In the phases that we are studying, the only important reactions are these two, and their ratios relative to one another have a few percentage differences, 1% or 2%, depending on the specific point of analysis.

It is also worth mentioning that, although it might be possible to predict distinguishable large separation curves when changing the S-factor, the process that governs this change is not linear, meaning that we might need a more complete seismic diagnostic to be able to estimate the S-factor from seismology. In this particular analysis we found that, even though the relative difference between **Ref** and **A** S-factors was bigger than between **Ref** and **B**, the results yielded that it would be much more difficult to observe the first difference than the second one using the current diagnostics.

These results, together with other tests we performed on the impact of the S-factor derivatives, namely comparing the presented models with modes **A** and **B** without the $S'(0)$ or $S''(0)$, also suggests that these first and second order terms of the series (equation 3) might have a non-negligible impact on the evolution of post MS stars. However, this observation still requires further detailed analysis before conclusions can be taken.

4. SUMMARY AND CONCLUSIONS

There are two main conclusions to note from this work. **(i)** Our results show that stars are sensitive to the S-factor of the pp reaction, specially after the MS phase and **(ii)** in certain conditions, this sensitivity can have measurable effects on the large separation of the star. In the post MS phase we have obtained a maximum mean difference of about 1.3μHz in the large separation between our reference NACRE model and the other two test models.

With our current setup, the results show that some different published values for the pp S-factor might have an impact in stellar modelling that could be measured if we happen to find a star with the conditions of bench points **2** or **3** [see section 2.2, figure 2 (bottom) and figure 6 (middle and bottom)], and have experimental data with less than 0.65μHz of mean uncertainty for point **2** and 0.45μHz for point **3**. There is the possibility, depending heavily on the equipments' specifications and on the target, that the new missions PLATO and TESS will be able to achieve this kind of accuracies, with observation times around 5 days. Other analyzed stages would require smaller error bars to distinguish the changes due to the S-factor.

Another feature of our simulations was that our first three bench models had a large separation pattern significantly different from the last two, which correlates with the existence of a convective envelope in models **4** and **5**, against a fully radiative envelope in the other models. This distinct pattern of $\Delta\nu_{n,0}$ could be useful in a more detailed study of the seismic characteristics of the star. We also have some hints that bench point **3** may be identifiable by the pattern in the large separation, but this requires a more detailed analysis in oscillation patterns before a conclusion can be drawn.

The results found for $1.5M_\odot$ stars may also be crucial for other stars since they affect the phase of evolution that has an analogous in $0.9M_\odot$, according to the most recent isochrones by the Yale-Potsdam Stellar Isochrones (YaPSI) group (Spada et al. 2017), and $7.0M_\odot$ stars (Girardi et al. 2000).

If corroborated by other independent analysis, our results may give a hint on a way to use measurements of eigenmodes in post main-sequence stars to put constrains on the currently only theoretical evaluation of the proton-proton cross section.

The work of IL was supported by grants from "Fundação para a Ciência e Tecnologia" and "Fundação Calouste Gulbenkian".

REFERENCES

Acharya, B., Carlsson, B. D., Ekström, A., Forssén, C., & Platter, L. 2016, Physics Letters B, 760, 584

Adelberger, E. G., Austin, S. M., Bahcall, J. N., et al. 1998, Reviews of Modern Physics, 70, 1265

Adelberger, E. G., García, A., Robertson, R. G. H., et al. 2011, Reviews of Modern Physics, 83, 195
Asteroseismic Modeling Portal (AMP) webpage, KIC 8026226 simulation by Metcalfe, T. 2014, AMP webpage
Angulo, C. et al 1999, NPA, 656, 3
Antoci, V. 2014, Precision Asteroseismology, 301, 333
Appourchaux, T., Chaplin, W. J., García, R. A., et al. 2012, A&A, 543, A54
Baglin, A., Auvergne, M., Barge, P., et al. 2006, The CoRoT Mission Pre-Launch Status - Stellar Seismology and Planet Finding, 1306, 33
Bahcall, J. N. 1989, Cambridge and New York, Cambridge University Press, 1989, 584 p.
Belkacem, K., Samadi, R., Mosser, B., Goupil, M.-J., & Ludwig, H.-G. 2013, Progress in Physics of the Sun and Stars: A New Era in Helio- and Asteroseismology, 479, 61
Bethe, H. A. 1939, Physical Review, 55, 434
Brito, A., & Lopes, I. 2017, MNRAS, 466, 2123
Brito, A., & Lopes, I. 2017, ApJ, 843, 75.
Brocato, E., Castellani, V., & Villante, F. L. 1998, MNRAS, 298, 557
Cantiello, M., Langer, N., Brott, I., et al. 2009, A&A, 499, 279
Carrier, F., Eggenberger, P., & Bouchy, F. 2005, A&A, 434, 1085
Caughlan, G. R., & Fowler, W. A. 1988, Atomic Data and Nuclear Data Tables, 40, 283
Chaplin, W. J., & Miglio, A. 2013, ARA&A, 51, 353
Chen, J.-W., Liu, C.-P., & Yu, S.-H. 2013, Physics Letters B, 720, 385
Cox, J. P. 1963, ApJ, 138, 487
Deheuvels, S., & Michel, E. 2011, A&A, 535, A91
Eddington, A. S. 1919, MNRAS, 79, 177
Eddington, A. S. 1920, The Observatory, 43, 341
Einstein, A. 1905, Annalen der Physik, 323, 639
Gilliland, R. L., Brown, T. M., Christensen-Dalsgaard, J., et al. 2010, PASP, 122, 131
Girardi, L., Bressan, A., Bertelli, G., & Chiosi, C. 2000, A&AS, 141, 371
Glatzel, W., & Kiriakidis, M. 1993, MNRAS, 262, 85
Gough, D. 1985, Nature, 314, 14-15
Gough, D. O., Merryfield, W. J., & Toomre, J. 1993, GONG 1992. Seismic Investigation of the Sun and Stars, 42, 257
Huber, D., Bedding, T. R., Stello, D., et al. 2011, ApJ, 743, 143
Kippenhahn, R., Weigert, A., & Weiss, A. 2012, Stellar Structure and Evolution: , Astronomy and Astrophysics Library. ISBN 978-3-642-30255-8. Springer-Verlag Berlin Heidelberg, 2012
Koch, D. G., Borucki, W. J., Basri, G., et al. 2010, ApJ, 713, L79-L86
Libbrecht, K. G. 1992, ApJ, 387, 712
Lochard, J., Samadi, R., & Goupil, M. J. 2005, A&A, 438, 939
Lopes, I., & Turck-Chieze, S. 1994, A&A, 290, 845
Lopes, I. P. 2001, A&A, 373, 916
Lopes, I. P., & Gough, D. 2001, MNRAS, 322, 473
Marcucci, L. E. & Schiavilla, R. & Viviani, M. 2013, PRL, 110, 19
Metcalfe, T S and Creevey, O L and Dogan, et al. 2014, ApJS, 214, 17
Molenda-Żakowicz, J., Sousa, S. G., Frasca, A., et al. 2013, MNRAS, 434, 1422
Morel, P., & Lebreton, Y. 2008, Ap&SS, 316, 61
Mosser, B. 2015, EAS Publications Series, 73, 3
Paxton, B., Bildsten, L., Dotter, A., et al. 2011, ApJS, 192, 3
Paxton, B., Cantiello, M., Arras, P., et al. 2013, ApJS, 208, 4
Paxton, B., Marchant, P., Schwab, J., et al. 2015, ApJS, 220, 15
Rauer, H., Catala, C., Aerts, C., et al. 2014, Experimental Astronomy, 38, 249
Ricker, G. R., Winn, J. N., Vanderspek, R., et al. 2014, Proc. SPIE, 9143, 914320
Ricker, G. R., Winn, J. N., Vanderspek, R., et al. 2015, Journal of Astronomical Telescopes, Instruments, and Systems, 1, 014003
Ryan, S. G., & Norton, A. J. 2010, Stellar Evolution and Nucleosynthesis by Sean G. Ryan and Andrew J. Norton. Cambridge University Press, 2010. ISBN: 9780521196093
Spada, F., Demarque, P., Kim, Y.-C., Boyajian, T. S., & Brewer, J. M. 2017, ApJ, 838, 161
Tassoul, M. 1980, ApJS, 43, 469
Tognelli, E. & DeglInnocenti, S. & Marcucci, L. E. & PradaMoroni, P. G. 2015, PLB, 742, 189-194
Townsend, R. H. D., & Teitler, S. A. 2013, MNRAS, 435, 3406
Unno, W., Osaki, Y., Ando, H., Saio, H., & Shibahashi, H. 1989, Nonradial oscillations of stars, Tokyo: University of Tokyo Press, 1989, 2nd ed.